Structural Variability of the Vanadium−Organodiphosphonate System: Hydrothermal Syntheses and Structural Characterizations of One-Dimensional, Two-Dimensional, and Three-Dimensional Phases

Grant Bonavia,[†] Robert C. Haushalter,[‡] C. J. O'Connor,[§] and Jon Zubieta*[,†]

Department of Chemistry, Syracuse University, Syracuse, New York 13244-4100, Department of Chemistry, University of New Orleans, New Orleans, Louisiana 70148, and NEC Research Institute, 4 Independence Way, Princeton, New Jersey 08540

Received February 29, 1996[⊗]

The hydrothermal chemistry of the $CsVO_3$/methylenediphosphonate system was investigated. Variations in reaction temperatures, heating times, and stoichiometries of reactants resulted in the isolation of mononuclear, one-, two-, and three-dimensional species: $Cs[VO(HO_3PCH_2PO_3H)_2(H_2O)]$ (**1**), $Cs[VO(HO_3PCH_2PO_3)]$ (**2**), $Cs[(VO)_2V(O_3PCH_2PO_3)_2(H_2O)_2]$ (**3**), and $[V(HO_3PCH_2PO_3)(H_2O)]$ (**4**), respectively. The structure of the anion of **1** consists of isolated V(IV) octahedra. Phase **2** adopts a chain structure constructed from corner-sharing V(IV) octahedra, forming infinite {−V═OV═O−} linkages. The layer structure of **3** contains trinuclear units of corner-sharing $\{VO_6\}$ octahedra with the central V site in the III oxidation state and V(IV) centers at the extremities of the cluster. The diphosphonate ligands serve to link neighboring trinuclear motifs into a layer structure three octahedra in depth. The Cs^+ cations occupy cavities *within the layers*, rather than the more common interlamellar positions. The structure of **4** consists of isolated $\{V(III)O_6\}$ octahedra linked by diphosphonate groups into a three-dimensional framework. Crystal data: for **1**, $CH_6O_7P_2V_{0.5}Cs$, monoclinic *C2*, $a = 10.991(2)$ Å, $b = 10.161(2)$ Å, $c = 7.445(1)$ Å, $\beta = 92.97(3)°$, $Z = 4$; for **2**, $CH_3O_7P_2VCs$, monoclinic *C2*, $a = 10.212(2)$ Å, $b = 10.556(2)$ Å, $c = 14.699(3)$ Å, $\beta = 94.57(2)°$, $Z = 8$; for **3**, $C_2H_8O_{16}P_4V_3Cs$, monoclinic *C2/m*, $a = 9.724(2)$ Å, $b = 8.136(2)$ Å, $c = 10.268(2)$ Å, $\beta = 103.75(3)°$, $Z = 2$; for **4**, $CH_5O_7P_2V$, monoclinic $P2_1/n$, $a = 5.341(1)$ Å, $b = 11.516(2)$ Å, $c = 10.558(2)$ Å, $\beta = 99.89(1)°$, $Z = 4$.

The recent expansion of metal organophosphonate chemistry reflects the practical applications to the design of solid materials with desirable bulk properties.[1−6] The vanadylorganophosphonates $[VO(RPO_3)]\cdot xH_2O$[7−9] and $[(VO)_2\{O_3PCH_2PO_3\}]\cdot 4H_2O$[10] exhibit structurally well-defined void spaces, permitting the intercalation of alcohols by substrate coordination to the vanadium centers of the VPO layer of the solid. As an approach to the design of selective oxidation catalysts,[11−13] we have sought to combine the modification of organic substituents of the organophosphonate, the thermal stability and reactivity of transition metal oxide units, the interplay of hydrophobic and hydrophilic domains, and substrate-specific recognition and incipient coordinative unsaturation of the vanadium sites. Based on our observations of major structural modifications in the layered V−O−RPO_3 phases by substituent modification and/or introduction of appropriate templates,[14−16] investigations of the chemistry of the vanadium−organodiphosphonate system, $V\{R(PO_3)_2H_{4-n}\}^{n-}$, in the hydrothermal reaction domain were initiated.

While solid state compounds have been conventionally prepared through high-temperature solid state reactions in which thermodynamic factors dominate, the use of hydrothermal techniques[17] allows the retention of the structural elements of the reactants in the product phase.[13] By exploiting hydrothermal synthesis, a variety of phases of the oxovanadium organodiphosphonate system, including a series of one-, two- and three-dimensional materials, have been reported.[18−20] For phases exhibiting negatively charged VOP networks, organoamine cations were required to induce crystallization. However, there is no *a priori* reason to expect that other cations, such as alkali metal, alkaline earths, or ammonium, should be excluded. In the course of our investigations of the chemistry of the $CsVO_3$/methylenediphosphonate system, the profound influence of

[†] Syracuse University.
[‡] NEC Research Institute.
[§] University of New Orleans.
[⊗] Abstract published in *Advance ACS Abstracts,* August 1, 1996.

(1) Snover, J. L.; Thompson, M. E. *J. Am. Chem. Soc.* **1994**, *116*, 765.
(2) Katz, H. E.; Wilson, W. L.; Scheller, G. *J. Am. Chem. Soc.* **1994**, *116*, 6636.
(3) Cao, G.; Hong, H. G.; Mallouk, T. G. *Acc. Chem. Res.* **1992**, *25*, 420.
(4) Alberti, G.; Costantino, U. In *Inclusion Compounds, Inorganic and Physical Aspects of Inclusion*; Atwood, J. L., Davies, J. E. D., MacNicol, D. D., Eds.; Oxford Science: Oxford, U.K., 1991; p 136.
(5) Clearfield, A. *Comments Inorg. Chem.* **1990**, *10*, 89.
(6) Zhang, Y.; Clearfield, A. *Inorg. Chem.* **1992,** *31*, 2821.
(7) Johnson, J. W.; Jacobson, A. J.; Butler, W. M.; Rosenthal, S. E.; Brody, J. F.; Lewandowski, J. T. *J. Am. Chem. Soc.* **1989**, *111*, 381.
(8) Huan, G. H.; Jacobson, A. J.; Johnson, J. W.; Corcoran, E. W., Jr. *Chem. Mater.* **1990**, *2*, 2.
(9) Huan, G.; Jacobson, A. J.; Johnson, J. W.; Goshorn, D. P. *Chem. Mater.* **1992**, *4*, 661.
(10) Huan, G. H.; Johnson, J. W.; Jacobson, A. J.; Merola, J. S. *J. Solid State Chem.* **1990**, *89*, 220.
(11) Mallouk, T. E.; Lee, H. *J. Chem. Educ.* **1990**, *67*, 829.
(12) Haushalter, R. C.; Mundi, L. A. *Chem. Mater.* **1992**, *4*, 31, and references cited therein.
(13) Stein, A.; Keller, S. W.; Mallouk, T. E. *Science* **1993**, *259*, 1558.
(14) $[Et_2NH_2][Me_2NH_2][(VO)_4(OH)_2(O_3PC_6H_5)_4]$: Khan, M. I.; Lee, Y.-S.; O'Connor, C. J.; Haushalter, R. C.; Zubieta, J. *J. Am. Chem. Soc.* **1994**, *116*, 4525.
(15) $[EtNH_3]_2[(VO)_3(H_2O)(O_3PC_6H_5)_4]$: Khan, M. I.; Lee, Y.-S.; O'Connor, C. J.; Haushalter, R. C.; Zubieta, J. *Inorg. Chem.* **1994**, *33*, 1953.
(16) $[Et_4N][(VO)_3(OH)(H_2O)(O_3PC_2H_5)_3]\cdot H_2O$: Khan, M. I.; Lee, Y.-S.; O'Connor, C. J.; Haushalter, R. C.; Zubieta, J. *Chem. Mater.* **1994**, *6*, 721.
(17) Figlarz, M. *Chem. Scr.* **1988**, *28*, 3.
(18) Soghomonian, V.; Chen, Q.; Haushalter, R. C.; Zubieta, J. *Angew. Chem., Int. Ed. Engl.* **1995**, *34*, 223.
(19) Soghomonian, V.; Diaz, R.; Haushalter, R. C.; O'Connor, C. J.; Zubieta, J. *Inorg. Chem.* **1995**, *34*, 4460.
(20) Soghomonian, V.; Haushalter, R. C.; Zubieta, J. *Chem. Mater.* **1995**, *7*, 1648.

S0020-1669(96)00224-8 CCC: $12.00

Table 1. Summary of the Crystallographic Data for the X-ray Studies of $Cs[VO(HO_3PCH_2PO_3H)_2(H_2O)]$ (**1**), $Cs[VO(HO_3PCH_2PO_3)]$ (**2**), $Cs[(VO)_2V(O_3PCH_2PO_3)_2(H_2O)_2]$ (**3**), and $[V(HO_3PCH_2PO_3)(H_2O)]$ (**4**)

	1	**2**	**3**	**4**
chem formula	$CH_6O_7P_2V_{0.5}Cs$	$C_2H_6O_{14}P_4V_2Cs_2$	$C_2H_8O_{16}P_4V_3Cs$	$C_2H_{10}O_{14}P_4V_2$
formula wght	348.4	746.8	697.7	483.9
a, Å	10.991(2)	10.212(2)	9.724(2)	5.341(1)
b, Å	10.161(2)	10.556(2)	8.136(2)	11.516(2)
c, Å	7.445(1)	14.699(3)	10.268(2)	10.558(2)
β, deg	92.97(3)	94.57(2)	103.75(3)	99.89(1)
space group	*C*2	*C*2	*C*2/*m*	$P2_1/n$
V, Å	830.3(2)	1579.5(8)	789.1(4)	639.7(2)
Z	4	4	2	2
D_{calc}, g cm^{-3}	2.787	3.141	2.936	2.512
D_{obs},[a] g cm^{-3}	2.75	3.16	2.95	2.47
μ, cm^{-1}	53.67	62.01	45.04	20.40
T, °C	−20	−20	−20	23
λ, Å		0.710 73 (Mo Kα)		
R[b]	0.048	0.046	0.060	0.047
R_w[c]	0.049	0.052	0.068	0.050

[a] Picnometry. [b] $R = \sum||F_o| - |F_c||/\sum|F_o|$. [c] $R_w = [\sum w(|F_o| - |F_c|)^2/\sum w|F_o|^2]^{1/2}$.

reaction conditions on product identity were manifested in the isolation and characterization of a molecular prototype, $Cs_2[(VO)(HO_3PCH_2PO_3H)_2(H_2O)]$ (**1**), the one-dimensional V(IV) species $Cs[(VO)(HO_3PCH_2PO_3)]$ (**2**), the mixed valence V(IV)/V(III) layered material $Cs[(VO)_2V(O_3PCH_2PO_3)_2(H_2O)_2]$ (**3**), and the reduced V(III) three-dimensional phase, $[V(HO_3PCH_2PO_3)(H_2O)]$ (**4**).

Experimental Section

The syntheses of **2**−**4** were carried out in thick-walled glass tubes under autogenous pressure. The reactants were stirred briefly before heating. The reaction tubes were filled to approximately 40% volume capacity. Reagents were purchased from Aldrich Chemical Co. and used without further purification.

Synthesis of $Cs_2[VO(HO_3PCH_2PO_3H)_2(H_2O)]$ (1). A solution of VCl_4 (0.15 mL, 1.66 M solution), methylenediphosphonate (0.035 g), CsCl (0.310 g), and H_2O (5 mL) in the mole ratio 1.00:0.80:7.39:1104 was stirred in a glass tube for 24 h at room temperature. Irregularly shaped blue-green blocks of **1** were isolated in 45% yield based on vanadium. IR (KBr pellet, cm^{-1}): 3348 (br), 2278 (br), 1682 (m), 1150 (m), 1022 (m), 964 (s), 931 (s), 796 (s). Anal. Calcd for $C_2H_{10}O_{14}P_2VCs_2$: C, 3.77; H, 1.57. Found: C, 4.01; H, 1.72.

Synthesis of $Cs[VO(HO_3PCH_2PO_3)]$ (2). A mixture of $CsVO_3$ (0.044 g), methylenediphosphonic acid (0.082 g), and H_2O (5 mL) in the mole ratio 1.00:2.46:1450 was heated in a autoclave for 48 h at 200 °C. Blue needles of **2** were isolated in 35% yield based on vanadium. IR (KBr pellet, cm^{-1}): 2982 (w), 2939 (m), 1121 (s), 1049 (s), 1007 (s), 964 (s), 897 (m), 762 (m). Anal. Calcd for $CH_3O_7P_2VCs$: C, 3.22; H, 0.80; V, 13.67. Found: C, 3.41; H, 0.65; V, 13.55.

Synthesis of $Cs[(VO)_2V(O_3PCH_2PO_3)_2(H_2O)_2]$ (3). A mixture of VCl_4 (0.10 mL, 1.66 M solution), CsCl (0.270 g), methylenediphosphonic acid (0.030 g), and H_2O (3 mL) in the mole ratio 1.00:9.68:1.02:994 was heated in an autoclave for 48 h at 270 °C. Green plates of **3** were isolated in 40% yield based on vanadium. IR (KBr pellet, cm^{-1}): 3441 (br), 3336 (br), 1637 (m), 1152 (s), 1032 (s), 892 (s), 790 (m). Anal. Calcd for $C_2H_8O_{16}P_4V_3Cs$: C, 3.44; H, 1.15; V, 21.92. Found: C, 3.56; H, 1.09; V, 21.72.

Synthesis of $[V(HO_3PCH_2PO_3)(H_2O)]$ (4). A mixture of VCl_4 (0.10 mL, 1.66 M solution), methylenediphosphonic acid (0.080 g), CsCl (0.310 g), and H_2O (3 mL) in the mole ratio 1.00:9.68:2.74:994 was heated in an autoclave for 48 h at 270 °C. Light green blocklike crystals of **4** were isolated in 30% yield based on vanadium. IR (KBr pellet, cm^{-1}): 3336 (s), 1631 (m), 1361 (m), 1201 (s), 1133 (m), 1032 (m), 990 (m), 931 (m), 838 (m). Anal. Calcd for $CH_5O_7P_2V$: C, 4.96; H, 2.07; V, 21.08. Found: C, 4.87; H, 2.00; V, 20.85.

X-ray Crystallographic Studies. Structural measurements for compounds **1**−**4** were performed on a Rigaku AFC5S diffractometer with graphite monochromated Mo Kα radiation (λ(MoKα) = 0.710 73 Å). The data were collected at a temperature of −20 ± 1 °C for **1**−**3** and 23 ± 1 °C for **4**, using the $\omega-2\theta$ scan technique to 45° in 2θ at scan speeds of 4−12°/min in ω. Crystallographic data for these phosphates are listed in Table 1.

The intensities of three standard reflections measured after every 150 reflections remained constant throughout the data collections. An empirical absorption correction, based on φ-scans, was applied to the data for **2**−**4**, while the program DIFABS[21] was used for **1**, resulting in transmission factors ranging from 0.56 to 1.00 for **1**, from 0.77 to 1.00 for **2**, from 0.72 to 1.00 for **3**, and from 0.64 to 1.00 for **4**. The data were corrected for Lorentz and polarization effects. The structures were solved by direct methods.[22] Vanadium and oxygen atoms were refined anisotropically. Neutral atom scattering factors were taken from Cromer and Waber,[23] and anomalous dispersion corrections were taken from those of Creagh and McAuley.[24] All calculations were performed using the SHELXTL[25] crystallographic software package.

Disorder problems were observed for several of the structures. In the case of **1**, the {V═O} unit is disordered along the crystallographic 2-fold axis, so as to occupy positions above and below the O_4 plane of the phosphonate oxygen donors. The relative populations of V1−O1 and V1A−O1A are approximately 0.70 and 0.30. This model refined to a conventional *R*-factor of 0.060 in the space group *C*2. Attempts to derive a structure in the centric alternative *C2/m* produced a model disordered about the mirror plane and giving unreasonable P−C and P−O distances, with a considerably larger residual. Furthermore, the reflection statistics were heavily weighted in favor of the acentric space group. The alternative acentric space group *Cm* failed to produce a reasonable model. On the bases of these observations, the refinement in *C2* was deemed appropriate. Refinement of the "inverted" structure resulted in significantly larger residuals, indicating that the absolute configuration chosen was correct.

Compound **2** also exhibits disorder of the vanadium sites along the {O−V═O} vectors. Once again, the vanadium sites occupy positions above and below the O_4 plane of the diphosphonate oxygen donors so as to produce the long−short V−O bond length alternations {O2═V1−O1═V2−} and {O2−V1A═O−V2A═} in relative populations of 0.75 and 0.25. The model refined in the acentric space group *C2* in an unexceptional fashion to give a conventional residual of 0.044. The reflection statistics again favored the acentric choice. More significantly, attempts to refine a model in the centric alternative *C2/m* produced unreasonable metrical parameters and temperature factors. The absolute configuration was checked by refining the inverted structure.

(21) Walker, N.; Stuart, D. *Acta Crystallogr. Sect. A 39* **1983**, 158.
(22) *teXsan: Texray Structural Analysis Package* (revised), Molecular Structure Corp,: The Woodlands, TX 1992.
(23) Cromer, D. T.; Waber, J. T. *International Tables for X-Ray Crystallography*; Kynoch Press: Birmingham, England, 1974; Vol. IV.
(24) Creagh, D. C.; McAuley, J. W. J. *International Tables for X-Ray Crystallography*; Kluwer Academic: Boston, 1992; Vol. C., Table 4.2.6.8.
(25) *SHELXTL PC*; Siemens Analytical X-Ray Instruments, Inc.: Madison, WI, 1990.

Table 2. Atomic Positional Parameters ($\times 10^4$) and Isotropic Temperature Factors (Å^2 $\times$ 10^3) for $Cs[VO(HO_3PCH_2PO_3H)_2(H_2O)]$ (**1**)

	x	y	z	*U*(eq)[a]
Cs(1)	0	0	0	40(2)
Cs(2)	0	5569(3)	0	43(2)
V(1)	0	−2213(17)	5000	33(1)
P(1)	2429(3)	−2257(14)	2583(5)	17(1)
P(2)	2761(4)	−1965(10)	6667(6)	25(3)
O(1)	0	−3846(14)	5000	70(6)
O(2)	0	−220(23)	4861(22)	23(6)
O(3)	1080(8)	−2150(33)	2941(12)	24(2)
O(4)	2676(12)	−1204(14)	1161(18)	28(3)
O(5)	2909(13)	−3585(16)	2055(21)	39(4)
O(6)	1421(8)	−2052(19)	6829(12)	19(2)
O(7)	3122(12)	−538(15)	6610(19)	36(4)
O(8)	3529(11)	−2647(11)	8240(16)	28(3)
C(1)	3189(18)	−2795(20)	4632(26)	35(5)

[a] Equivalent isotropic *U* defined as one-third of the trace of the orthogonalized $\mathbf{U}_{ij}$ tensor.

Table 3. Atomic Positional Parameters ($\times 10^4$) and Isotropic Temperature Factors (Å^2 $\times$ 10^3) for $Cs[VO(HO_3PCH_2PO_3)]$ (**2**)

	x	y	z	*U*(eq)[a]
Cs(1)	0	8843(2)	5000	39(1)
Cs(2)	0	8782	0	23(1)
Cs(3)	0	4673(1)	5000	22(1)
Cs(4)	0	4630(2)	0	41(1)
V(1A)	−35(5)	6440(7)	2531(3)	11(1)
V(1B)	75(22)	6443(31)	7558(14)	13(7)
V(2A)	2179(5)	9170(5)	2456(3)	9(1)
V(2B)	2768(11)	4186(12)	7438(7)	6(3)
P(1)	2290(3)	12021(3)	13338(2)	10(1)
P(2)	2290(3)	11794(3)	11348(2)	10(1)
P(3)	−2790(3)	6535(3)	8332(2)	11(1)
P(4)	2223(3)	11756(3)	6346(2)	11(1)
O(1)	737(7)	8570(8)	12438(5)	13(2)
O(2)	632(7)	5046(8)	7424(6)	15(2)
O(3)	1222(7)	7260(9)	6635(6)	14(2)
O(4)	1972(7)	10609(9)	3354(6)	12(2)
O(5)	1705(8)	2704(8)	4133(6)	17(2)
O(6)	1217(7)	7023(9)	8558(5)	12(2)
O(7)	1974(7)	10394(8)	11447(6)	13(2)
O(8)	1682(7)	12332(9)	10444(6)	29(3)
O(9)	−1330(7)	6184(8)	8369(6)	14(2)
O(10)	−2997(7)	7978(9)	8341(6)	13(2)
O(11)	1554(7)	10921(8)	9114(6)	13(2)
O(12)	1314(7)	6410(9)	3580(6)	14(2)
O(13)	2018(7)	3183(9)	6446(6)	14(2)
O(14)	1542(7)	11302(9)	5438(6)	16(2)
C(1)	1596(10)	12660(11)	12262(8)	11(3)
C(2)	1489(10)	10954(12)	7243(9)	13(3)

[a] Equivalent isotropic *U* defined as one-third of the trace of the orthogonalized $\mathbf{U}_{ij}$ tensor.

In the case of compound **3**, the Cs^+ cations are disordered about the inversion centers at 0, 0, 0 and $^1/_2$, $^1/_2$, 0. The refinement was otherwise unexceptional, and the choice of the centric space group *C2/m* was unambiguous.

Atomic positional parameters and isotropic temperature factors for **1**−**4** are listed in Tables 2−5, respectively. Selected bond lengths and angles for **1**−**4** are presented in Tables 6−9, respectively.

Magnetic Studies. The magnetic susceptibility data were recorded on polycrystalline samples of **2**−**4** over the 1.7−300 K temperature range using a Quantum Design MPMS-5S SQUID susceptometer. The temperature dependent magnetic data were measured at a magnetic field of 1000 G. Measurement and calibration techniques have been reported elsewhere.[26]

Results and Discussion

Syntheses. Under conventional conditions, the reaction of an aqueous solution containing V(IV), from the hydrolysis of VCl_4, with methylenediphosphonic acid, in the presence of Cs^+ cations, yields blue-green crystals of the Cs^+ salt of the mononuclear anionic complex $[VO(HO_3PCH_2PO_3H)(H_2O)]^{2-}$. The vanadium starting material must be present in the reduced V(IV) form to obtain isolatable products; reactions with $CsVO_3$ or V_2O_5 as precursors failed to produce monophasic products containing diphosphonate coordinated metal, rather producing only uncharacterized mixtures. The infrared spectrum of $Cs_2[VO(HO_3PCH_2PO_3H)(H_2O)]$ (**1**) exhibited a broad band at 3348 cm^{-1} assigned to ν(OH) of the coordinated water and a series of bands in the 900−1200 cm^{-1} region, specifically 931,

Table 4. Atomic Positional Parameters ($\times 10^4$) and Isotropic Temperature Factors (Å^2 $\times$ 10^3) for $Cs[(VO)_2V(O_3PCH_2PO_3)_2(H_2O)_2]$ (**3**)

	x	y	z	*U*(eq)[a]
Cs	631(3)	0	277(2)	37(1)
V(1)	7637(3)	0	3024(3)	12(1)
V(2)	5000	0	0	23(2)
P(1)	4719(3)	1802(4)	2656(3)	27(1)
O(1)	4442(7)	1716(8)	1131(6)	18(2)
O(2)	3691(7)	−1726(9)	−3316(6)	22(2)
O(3)	882(10)	−1649(13)	−3111(8)	37(4)
O(4)	3509(10)	0	−1253(9)	14(3)
O(5)	1663(12)	0	−5166(11)	30(5)
C(1)	6095(21)	0	−3145(21)	37(5)

[a] Equivalent isotropic *U* defined as one-third of the trace of the orthogonalized $\mathbf{U}_{ij}$ tensor.

Table 5. Atomic Positional Parameters ($\times 10^4$) and Isotropic Temperature Factors (Å^2 $\times$ 10^3) for $[V(HO_3PCH_2PO_3)(H_2O)]$ (**4**)

	x	y	z	*U*(eq)[a]
V(1)	0	0	5000	8(1)
V(2)	0	5000	5000	8(1)
P(1)	655(4)	305(2)	1871(2)	7(1)
P(2)	2224(3)	2521(2)	6194(2)	9(1)
O(1)	963(10)	264(5)	3326(5)	15(2)
O(2)	2987(10)	−170(5)	1426(5)	14(2)
O(3)	−1768(10)	−366(5)	1280(5)	11(2)
O(4)	351(10)	3304(5)	5373(5)	13(2)
O(5)	2397(10)	1301(5)	5660(5)	11(2)
O(6)	1478(10)	2394(5)	7576(5)	15(2)
O(7)	3114(10)	−1071(5)	5408(6)	17(2)
C(1)	346(15)	1817(7)	1378(8)	13(2)

[a] Equivalent isotropic *U* defined as one-third of the trace of the orthogonalized $\mathbf{U}_{ij}$ tensor.

Table 6. Selected Bond Lengths (Å) and Angles (deg) for $Cs[VO(HO_3PCH_2PO_3H)_2(H_2O)]$ (**1**)

V(1)−O(1)	1.660(17)	V(1)−O(2)	2.027(20)
V(1)−O(3)	1.988(9)	V(1)−O(6)	2.025(9)
V(1)−O(3A)	1.988(9)	V(1)−O(6A)	2.025(9)
P(1)−O(3)	1.524(10)	P(1)−O(4)	1.539(17)
P(1)−O(5)	1.508(20)	P(1)−C(1)	1.787(20)
P(2)−O(6)	1.487(10)	P(2)−O(7)	1.504(18)
P(2)−O(8)	1.569(13)	P(2)−C(1)	1.817(21)
O(1)−V(1)−O(2)	177.1(15)	O(1)−V(1)−O(3)	91.8(11)
O(2)−V(1)−O(3)	85.8(16)	O(1)−V(1)−O(6)	94.6(7)
O(2)−V(1)−O(6)	87.2(12)	O(3)−V(1)−O(6)	92.6(4)
O(1)−V(1)−O(3A)	91.8(11)	O(2)−V(1)−O(3A)	90.5(16)
O(3)−V(1)−O(3A)	176.3(21)	O(6)−V(1)−O(3A)	87.1(4)
O(1)−V(1)−O(6A)	94.6(7)	O(2)−V(1)−O(6A)	83.5(12)
O(3)−V(1)−O(6A)	87.1(4)	O(6)−V(1)−O(6A)	170.8(14)
O(3A)−V(1)−O(6A)	92.6(4)	O(3)−P(1)−O(4)	106.2(12)
O(3)−P(1)−O(5)	117.8(15)	O(4)−P(1)−O(5)	111.4(8)
O(5)−P(1)−C(1)	106.8(9)	O(6)−P(2)−O(7)	108.9(10)
O(6)−P(2)−O(8)	114.2(8)	O(7)−P(2)−O(8)	108.3(7)
O(6)−P(2)−C(1)	109.9(9)	O(7)−P(2)−C(1)	110.1(9)
O(8)−P(2)−C(1)	105.4(9)	V(1)−O(3)−P(1)	139.3(6)
V(1)−O(6)−P(2)	133.1(6)	P(1)−C(1)−P(2)	116.1(11)

(26) O'Connor, C. J. *Prog. Inorg. Chem.* **1982**, *29*, 203.

Table 7. Selected Bond Lengths (Å) and Angles (deg) for $Cs[VO(HO_3PCH_2PO_3)]$ (**2**)

V(1)−O(1)	2.390(11)	V(1)−O(2)	1.985(9)
V(1)−O(3)	1.989(10)	V(1)−O(2)	1.596(11)
V(1)−O(9)	2.016(10)	V(1)−O(6)	2.022(9)
V(2)−O(1)	1.601(9)	V(2)−O(4)	2.034(11)
V(2)−O(7)	1.966(10)	V(2)−O(2)	2.413(9)
V(2)−O(13)	2.038(10)	V(2)−O(10)	1.952(10)
P(1)−O(3)	1.538(7)	P(1)−C(1)	1.810(11)
P(1)−O(5)	1.534(10)	P(1)−O(4)	1.526(10)
P(2)−O(8)	1.531(9)	P(2)−O(7)	1.523(9)
P(2)−O(6)	1.539(7)	P(2)−C(1)	1.815(12)
P(3)−O(10)	1.538(10)	P(3)−O(9)	1.533(8)
P(3)−C(2)	1.814(13)	P(3)−O(11)	1.521(9)
P(4)−C(2)	1.782(13)	P(4)−O(14)	1.531(9)
P(4)−O(13)	1.529(10)	P(4)−O(12)	1.534(8)
O(12)−V(1)−O(1)	81.3(4)	O(12)−V(1)−O(2)	101.3(5)
O(1)−V(1)−O(2)	176.8(4)	O(12)−V(1)−O(3)	87.0(4)
O(1)−V(1)−O(3)	81.2(4)	O(2)−V(1)−O(3)	97.1(5)
O(12)−V(1)−O(6)	162.5(5)	O(1)−V(1)−O(6)	81.2(4)
O(2)−V(1)−O(6)	96.2(5)	O(3)−V(1)−O(6)	90.1(4)
O(12)−V(1)−O(9)	92.0(4)	O(1)−V(1)−O(9)	80.8(4)
O(2)−V(1)−O(9)	100.9(5)	O(3)−V(1)−O(9)	161.9(5)
O(6)−V(1)−O(9)	85.5(4)	O(4)−V(2)−O(1)	99.4(4)
O(4)−V(2)−O(2)	79.1(3)	O(1)−V(2)−O(2)	176.7(5)
O(4)−V(2)−O(7)	89.4(4)	O(1)−V(2)−O(7)	101.8(4)
O(2)−V(2)−O(7)	81.1(4)	O(4)−V(2)−O(10)	160.5(4)
O(1)−V(2)−O(10)	99.9(5)	O(2)−V(2)−O(10)	81.5(4)
O(7)−V(2)−O(10)	89.7(4)	O(4)−V(2)−O(13)	85.7(4)
O(1)−V(2)−O(13)	97.0(4)	O(2)−V(2)−O(13)	80.0(3)
O(7)−V(2)−O(13)	161.1(4)	O(10)−V(2)−O(13)	88.9(4)
C(1)−P(1)−O(3)	106.2(5)	C(1)−P(1)−O(4)	108.0(5)
O(3)−P(1)−O(4)	111.8(5)	C(1)−P(1)−O(5)	109.9(5)
O(3)−P(1)−O(5)	110.3(5)	O(4)−P(1)−O(5)	110.5(5)
O(7)−P(2)−O(8)	111.6(5)	O(7)−P(2)−C(1)	108.7(5)
O(8)−P(2)−C(1)	107.5(5)	O(7)−P(2)−O(6)	111.1(5)
O(8)−P(2)−O(6)	110.5(5)	C(1)−P(2)−O(6)	107.3(5)
O(9)−P(3)−O(10)	111.9(5)	O(9)−P(3)−O(11)	110.8(5)
O(10)−P(3)−O(11)	110.3(5)	O(9)−P(3)−C(2)	106.0(5)
O(10)−P(3)−C(2)	107.2(5)	O(11)−P(3)−C(2)	110.5(5)
O(14)−P(4)−C(2)	107.9(5)	O(14)−P(4)−O(12)	111.1(5)
C(2)−P(4)−O(12)	107.4(5)	O(14)−P(4)−O(13)	109.6(5)
C(2)−P(4)−O(13)	109.1(5)	O(12)−P(4)−O(13)	111.6(5)
V(1)−O(1)−V(2)	132.7(5)	V(2)−O(2)−V(1)	135.2(6)
V(1)−O(3)−P(1)	121.9(8)	V(2)−O(4)−P(1)	133.3(6)
V(1)−O(6)−P(2)	124.1(9)	P(2)−O(7)−V(2)	131.1(6)
V(1)−O(9)−P(3)	134.7(9)	P(3)−O(10)−V(2)	124.6(5)
V(1)−O(12)−P(4)	131.6(5)	V(2)−O(13)−P(4)	124.7(6)
P(1)−C(1)−P(2)	108.0(6)	P(4)−C(2)−P(3)	109.1(6)

1022, and 1150 cm^{-1}, attributed to ν(P—O) of the diphosphonate ligands. The strong band at 964 cm^{-1} is associated with ν(V═O).

In contrast to the conventional synthesis affording **1**, the solid phases **2**−**4** could be isolated only by employing the techniques of hydrothermal synthesis.[27−30] While the hydrothermal method has been a well-documented means of synthesizing zeolites,[31] only in recent times has it been extended to the preparation of metastable materials containing oxometal polyhedra and framework element (P, As, Al) tetrahedra.[8−12,30,32,33]

When temperatures in the 150−270 °C range under autogenous pressures are employed, rather than the high-temperature methods now routinely used in solid state chemistry, self-assembly from simple molecular precursors of metastable phases which retain the bond relationships between most of the constituent atoms may be accomplished. A variety of starting materials may be introduced since most species are soluble under these conditions of synthesis. Furthermore, a variety of templating cations may be employed to direct the organization of the solid and to induce crystallization, since templates of appropriate size or geometry may be selected from the reaction mixture to fill the crystal vacancies. These features of the synthesis were exploited previously in the preparation of the series of one-, two- and three-dimensional materials: $[H_2pip][(VO)(O_3PCH_2PO_3)]$ (pip = piperazine, $[H_2en][(VO)(O_3PCH_2CH_2PO_3)]$ (en = ethylenediamine), and $[H_2en][(VO)_4(OH)_2$-

Table 8. Selected Bond Lengths (Å) and Angles (deg) for $Cs[(VO)_2V(O_3PCH_2PO_3)_2(H_2O)_2]$ (**3**)

V(1)−O(2A)	1.978(7)	V(1)−O(2)	1.978(7)
V(1)−O(3A)	1.954(10)	V(1)−O(3)	1.954(10)
V(1)−O(5)	2.142(11)	V(1)−O(4)	1.783(9)
V(2)−O(4)	2.016(8)	V(2)−O(1)	1.973(7)
V(2)−O(1B)	1.973(7)	V(2)−O(1A)	1.973(7)
V(2)−O(4A)	2.016(8)	V(2)−O(1C)	1.973(7)
P(1)−O(2)	1.535(7)	P(1)−O(1)	1.526(7)
P(1)−C(1)	1.793(10)	P(1)−O(3)	1.510(9)
O(2)−V(1)−O(2A)	90.5(4)	O(2)−V(1)−O(3)	90.4(4)
O(2)−V(1)−O(3A)	168.7(3)	O(3)−V(1)−O(3A)	86.7(6)
O(2)−V(1)−O(4)	93.0(3)	O(3)−V(1)−O(4)	98.2(3)
O(2)−V(1)−O(5)	84.5(3)	O(3)−V(1)−O(5)	84.4(3)
O(4)−V(1)−O(5)	176.4(5)	O(1)−V(2)−O(4)	91.7(3)
O(1)−V(2)−O(1A)	180.0(1)	O(4)−V(2)−O(1)	88.3(3)
O(1)−P(1)−O(2)	111.4(4)	O(1)−P(1)−O(3)	111.7(4)
O(2)−P(1)−O(3)	108.7(5)	O(1)−P(1)−C(1)	105.5(7)
O(2)−P(1)−C(1)	108.0(6)	O(3)−P(1)−C(1)	111.5(7)
V(2)−O(1)−P(1)	129.1(4)	V(1)−O(2)−P(1)	125.9(4)
V(1)−O(3)−P(1)	153.4(5)	V(2)−O(4)−V(1)	136.2(6)
P(1)−C(1)−P(1A)	109.6(12)		

Table 9. Selected Bond Lengths (Å) and Angles (deg) for $[V(HO_3PCH_2PO_3)(H_2O)]$ (**4**)

V(1)−O(1)	1.947(6)	V(1)−O(5)	2.016(5)
V(1)−O(7)	2.056(6)	V(1)−O(1A)	1.947(6)
V(1)−O(5A)	2.016(5)	V(1)−O(7A)	2.056(6)
V(2)−O(4)	1.995(6)	V(2)−O(2)	2.004(6)
V(2)−O(2A)	2.004(6)	V(2)−O(3)	2.045(5)
V(2)−O(3A)	2.045(5)	V(2)−O(4A)	1.995(6)
P(1)−O(1)	1.518(6)	P(1)−O(2)	1.507(6)
P(1)−O(3)	1.544(6)	P(1)−C(1)	1.816(8)
P(2)−O(4)	1.506(6)	P(2)−O(5)	1.523(6)
P(2)−O(6)	1.584(6)	P(2)−C(1)	1.813(8)
O(1)−V(1)−O(5)	86.9(2)	O(1)−V(1)−O(7)	87.3(2)
O(5)−V(1)−O(7)	86.0(2)	O(1)−V(1)−O(1A)	180.1(1)
O(5)−V(1)−O(1A)	93.1(2)	O(7)−V(1)−O(1A)	92.7(2)
O(1)−V(1)−O(5A)	93.1(2)	O(5)−V(1)−O(5A)	180.0(1)
O(7)−V(1)−O(5A)	94.0(2)	O(1A)−V(1)−O(5A)	86.9(2)
O(1)−V(1)−O(7A)	92.7(2)	O(5)−V(1)−O(7A)	94.0(2)
O(7)−V(1)−O(7A)	180.0(1)	O(1A)−V(1)−O(7A)	87.3(2)
O(5A)−V(1)−O(7A)	86.0(2)	O(4)−V(2)−O(2)	90.5(2)
O(4)−V(2)−O(2A)	89.5(2)	O(2)−V(2)−O(2A)	180.0(1)
O(4)−V(2)−O(3)	88.2(2)	O(2)−V(2)−O(3)	89.1(2)
O(2A)−V(2)−O(3)	90.9(2)	O(4)−V(2)−O(3A)	91.8(2)
O(2)−V(2)−O(3A)	90.9(2)	O(2A)−V(2)−O(3A)	89.1(2)
O(3)−V(2)−O(3A)	180.0(1)	O(4)−V(2)−O(4A)	180.0(1)
O(2)−V(2)−O(4A)	89.5(2)	O(2A)−V(2)−O(4A)	90.5(2)
O(3)−V(2)−O(4A)	91.8(2)	O(3A)−V(2)−O(4A)	88.2(2)
O(1)−P(1)−O(2)	110.6(3)	O(1)−P(1)−O(3)	109.3(3)
O(2)−P(1)−O(3)	111.8(3)	O(1)−P(1)−C(1)	108.0(4)
O(2)−P(1)−C(1)	107.4(4)	O(3)−P(1)−C(1)	109.6(3)
O(4)−P(2)−O(5)	114.5(3)	O(4)−P(2)−O(6)	109.8(3)
O(5)−P(2)−O(6)	107.3(3)	O(4)−P(2)−C(1)	108.5(3)
O(5)−P(2)−C(1)	108.3(3)	O(6)−P(2)−C(1)	108.2(3)
V(1)−O(1)−P(1)	157.5(4)	P(1)−O(2)−V(2)	141.0(3)
P(1)−O(3)−V(2)	135.8(3)	V(2)−O(4)−P(2)	136.9(3)
V(1)−O(5)−P(2)	137.6(3)	P(1)−C(1)−P(2)	118.1(5)

(27) Figlarz, M. *Chem. Scr.* **1988**, *28*, 3.
(28) Rouxel, J. *Chem. Scr.* **1988**, *28*, 33.
(29) Laudise, R. A. *Chem. Eng. News* **1987**, *65* (Sept 8), 30.
(30) Gopalakrishnan, J. *Chem. Mater.* **1995**, *7*, 1265.
(31) Davis, M. E.; Lobo, R. F. *Chem. Mater.* **1992**, *4*, 756.
(32) Soghomonian, V.; Chen, Q.; Haushalter, R. C.; Zubieta, J.; O'Connor, C. J. *Science* **1993**, *259*, 1596.
(33) Numerous examples of hydrothermal syntheses of solids incorporating the oxovanadium core have appeared in recent years, among others: (a) Bu, X.; Feng, P.; Stucky, G. *J. Chem. Soc., Chem. Commun.* **1995**, 1337. (b) Riou, D.; Férey, C. *J. Solid State Chem.* **1995**, *120*, 137.

$(H_2O)_2(O_3PCH_2CH_2CH_2PO_3)_2]\cdot 4H_2O$, respectively.[18] However, it became abundantly clear that reaction conditions as well as the nature of the template profoundly influence the product composition and structure. For example, modification of reaction temperature and duration provided a unique stair-step product $[H_2pip][(VO)_2(O_3PCH_2CH_2CH_2PO_3H)_2]$;[19] moreover, organic cations could be excluded altogether, as in the hydronium-containing product, $(H_3O)_2[(VO)V_2(OH)_2(O_3PCH_2CH_2PO_3)_2]\cdot H_2O$;[20] and complete reduction of the vanadium sites to the V(III) state may be accomplished, as for $(H_3O)[V_3(O_3PCH_2CH_2PO_3)(HO_3PCH_2CH_2PO_3H)_3]$.[20] Consequently, the remarkable structural versatility of the organodiphosphonate group in linking vanadium polyhedra into solids whose composition and dimensionality are determined by specific reaction conditions was exploited in the investigation of synthetic parameter space for the cesium cation−vanadium− methylenediphosphonic acid system.

Monophasic crystalline materials **2**−**4** could be isolated only at relatively high temperatures, 200−270 °C. The one-dimensional material, $Cs[(VO)(HO_3PCH_2PO_3)]$ (**2**), was prepared at the lower limit of this temperature range, while **3** and **4** could be isolated only at 270 °C. Curiously, the only difference in synthetic conditions for these latter materials was the amount of diphosphonate introduced, reflected in the VCl_4:$H_2O_3PCH_2PO_3H_2$:CsCl:H_2O mole ratios of 1.00:1.02:9.68:994 and 1.00:2.74:9.68:994 for **3** and **4**, respectively. Such pronounced dependence on reaction conditions appears to be a characteristic feature of the hydrothermal chemistry of vanadium-phosphate and vanadium−organophosphonate systems.[34]

The infrared spectrum of **2** exhibits the features at 1007, 1049, and 1121 cm^{-1} characteristic of ν(P−O) of the diphosphonate groups and a strong band at 964 cm^{-1} attributed to ν(V═O). The absence of features in the 3000−3300 cm^{-1} region confirmed that the material did not incorporate water.

The spectra of $Cs[(VO)_2V(O_3PCH_2PO_3)_2(H_2O)_2]$ (**3**) and $[V(HO_3PCH_2PO_3)(H_2O)]$ (**4**), likewise, possessed a series of bands in the 1000−1200 cm^{-1} region, consistent with ν(P−O). The appearance of broad, medium intensity features for both **3** and **4** in the 3300−3400 cm^{-1} region confirmed the presence of coordinated water. The infrared spectrum of **3** did not exhibit a characteristic ν(V═O) band in the 950−1000 cm^{-1} range; however, the observation of a strong, sharp band at 892 cm^{-1} suggested the existence of {V═O−V} linkages, which was subsequently confirmed by the X-ray crystallographic studies. The absence of strong bands in the 800−1000 cm^{-1} region of **4** is consistent with the assignment of the V(III) oxidation state and consequently the absence of {V═O} moieties.

Descriptions of the Structures. The structure of $Cs_2[(VO)(HO_3PCH_2PO_3H)_2(H_2O)]$ (**1**) consists of discrete Cs^+ cations and $[(VO)(HO_3PCH_2PO_3H)_2(H_2O)]^{2-}$ anions. As shown in Figure 1, the V(IV) site exhibits distorted octahedral geometry, defined by the terminal oxo-group, an aquo ligand, and four oxygen donors from two methylenediphosphonate ligands, each adopting the bidentate coordination mode. Charge balance considerations establish that the ligand is doubly protonated $(HO_3PCH_2PO_3H)^{2-}$, an observation confirmed by the P−O bond distances of 1.55(1) Å (av) and 1.51(1) Å (av), for the protonated {P−OH} sites and the pendant {P═O} units, respectively. Valence bond calculations confirm that the vanadium is in the IV oxidation state.[35]

The isolation of a mononuclear species was unexpected given the pronounced tendency of organophosphonate groups to bridge

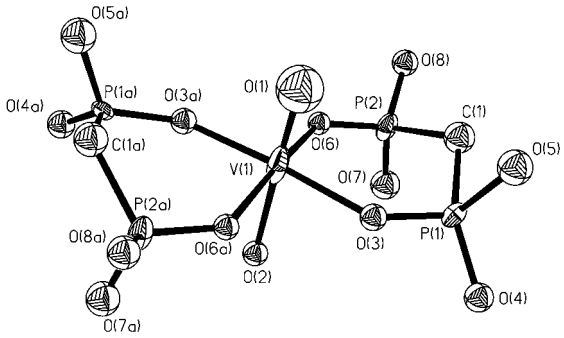

Figure 1. View of the structure of the anion of $Cs_2[(VO)(HO_3PCH_2PO_3H)_2(H_2O)]$ (**1**), showing the atom-labeling scheme.

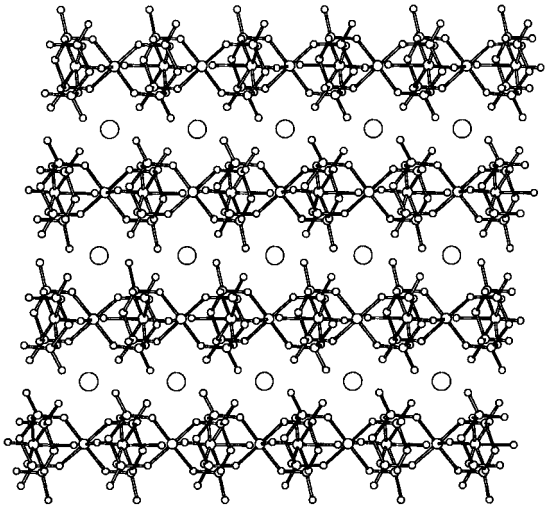

Figure 2. View of the anionic chains of $Cs[VO(HO_3PCH_2PO_3)]$ (**2**). The Cs^+ cations occupy positions between the strands.

metal sites in the construction of complex binuclear and oligomeric species.[35,36] However, the pendant {P−OH} and {P═O} units are disposed so as to adopt a bisbidentate bridging mode to an adjacent metal center and thus to provide oligomers or solids under appropriate conditions of synthesis and crystallization. In this sense, the mononuclear species **1** provides a structural prototype for the construction of the solid phases. Indeed, the structural motif adopted by the anions of **1** is a recurrent theme in the structures of **2**−**4**.

As illustrated in Figure 2, the structure of **2** consists of discrete Cs^+ cations occupying the vacancies between undulating negatively charged chains, $[VO(HO_3PCH_2PO_3)]$. The vanadium centers of the anionic chain adopt distorted octahedral geometry, defined by two *trans* oxo-groups and four oxygen donors from two bidentate methylenediphosphonate groups. The one-dimensional linkage may be described in terms of corner-sharing VO_6 octahedra, forming {−V═O−V═} chains with alternating long−short {V−O} distances. Each vanadium octahedron shares two bisbidentate diphosphonate groups, one with each of two adjacent vanadium centers, thus introducing bends into the {−V═O−V═} chains with a V−O−V angle of 135.2(6)°.

The bisbidentate coordination mode adopted by the methylenediphosphonate ligand has been previously documented in the chain structures $[Li(H_2O)_3][Tc(OH)(O_3PCH_2PO_3)]$,[37] $Na_4[W_2O_6(O_3PCH(R)PO_3)]\cdot 11H_2O$,[38] and $(H_2pip)[VO(O_3PCH_2PO_3)]$.[18] While the Tc and W species also adopt a structure

(34) Zubieta, J. *Comments on Inorg. Chem.* **1994**, *16*, 153, and references cited therein.
(35) Brown, I. D. In *Structure and Bonding in Crystals*; O'Keefe, M., Navrotsky, A, Eds.; Academic Press: New York, 1981; Vol. II, p 1.
(36) Khan, M. I.; Zubieta, J. *Prog. Inorg. Chem.* **1995**, *43*, 1, and references cited therein.
(37) Libson, K.; Deutsch, E.; Barnett, B. L. *J. Can. Chem. Soc.* **1980**, *102*, 2476.
(38) Kortz, U.; Pope, M. T. *Inorg. Chem.* **1995**, *34*, 38848.

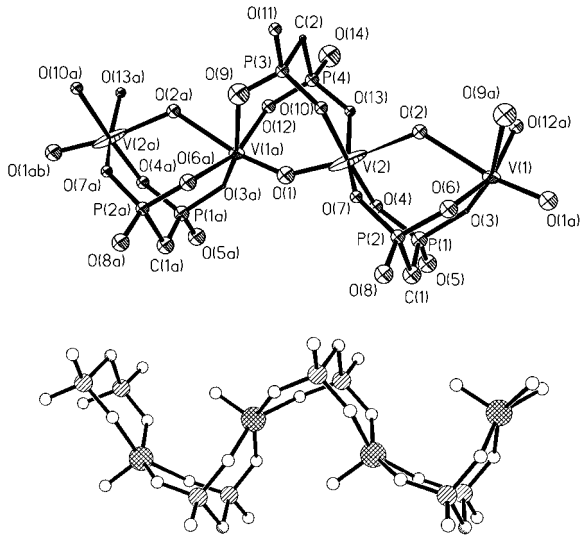

Figure 3. (a, top) View of a single anionic chain of **2**, showing the atom-labeling scheme. (b, bottom) View of the 1-D chains of $[H_2pip][VO(O_3PCH_2PO_3)]$. The distance from a vanadium site to the oxo-group of an adjacent vanadium is 3.43 Å.

constructed from corner-sharing $\{MO_6\}$ octahedra, the latter oxovanadium species is unique, exhibiting isolated $\{VO_5\}$ square pyramids with no {V—O—V} linkages. The structure of **2** is readily derived from that of the $[VO(O_3PCH_2PO_3)]^{2-}$ by folding along the O···O vectors, defined by the oxygen donors of a methylenediphosphonate ligand, so as to contract the V—O—P angle and consequently the angles between O_4-(phosphonate) planes of adjacent vanadium octahedra. The anionic chains of **2** and $[VO(O_3PCH_2PO_3)]^{2-}$ are compared in Figure 3, and relevant metrical parameters are given in Table 10.

It is noteworthy that the organodiphosphonate units of **2** adopt a singly protonated mode $(HO_3PCH_2PO_3)^{3-}$, unlike the fully deprotonated types found for $[Tc(OH)(O_3PCH_2PO_3)]^-$, $[W_2O_6(O_3PCH(R)PO_3)]^{4-}$, and $(H_2pip)[VO(O_3PCH_2PO_3)]$. Ligand protonation in **2** is consistent with charge balance considerations; however, the pendant P—O distances, which fall in the narrow range in the range 1.521−1.534 Å, do not allow identification of the protonation sites.

The Cs^+ cations of **2** adopt irregular geometries in the interstrand vacancies. As seen in Figure 2, the Cs^+ positions are localized within channels defined by the pendant {P═O} and {P—OH} groups of adjacent chains which project into the interchain region.

As shown in Figure 4, the unprecedented structure of $Cs[(VO)_2V(O_3PCH_2PO_3)_2(H_2O)_2]$ (**3**) consists of Cs^+ cations encapsulated within channels of a two-dimensional vanadium−oxygen−methylenediphosphonate network. The network is constructed from $\{(VO)_2V(O_3PCH_2PO_3)_2(H_2O)_2\}^-$ building blocks, containing an unique mixed valence V(IV)/V(III) trinuclear unit of corner-sharing $\{VO_6\}$ octahedra. Valence sum calculations unambiguously identify the two outermost vanadium centers as V(IV) sites and the central vanadium as a V(III) site. The V(IV) octahedra are defined by a terminal oxo-group, a *trans* aquo ligand, two oxygen donors from a methylenediphosphonate group in the bisbidentate mode within the trinuclear motif, and one oxygen donor from each of two methylenediphosphonate groups from two adjacent trinuclear motifs. The central V(III) octahedron consists of two *trans* oxo-groups and four oxygen donors from each of two methylenediphosphonate ligands in the bisbidentate mode with respect to the $[(VO)_2V(O_3PCH_2PO_3)_2(H_2O)]^-$ unit.

Since each V(IV) site directs its oxo-group toward the central

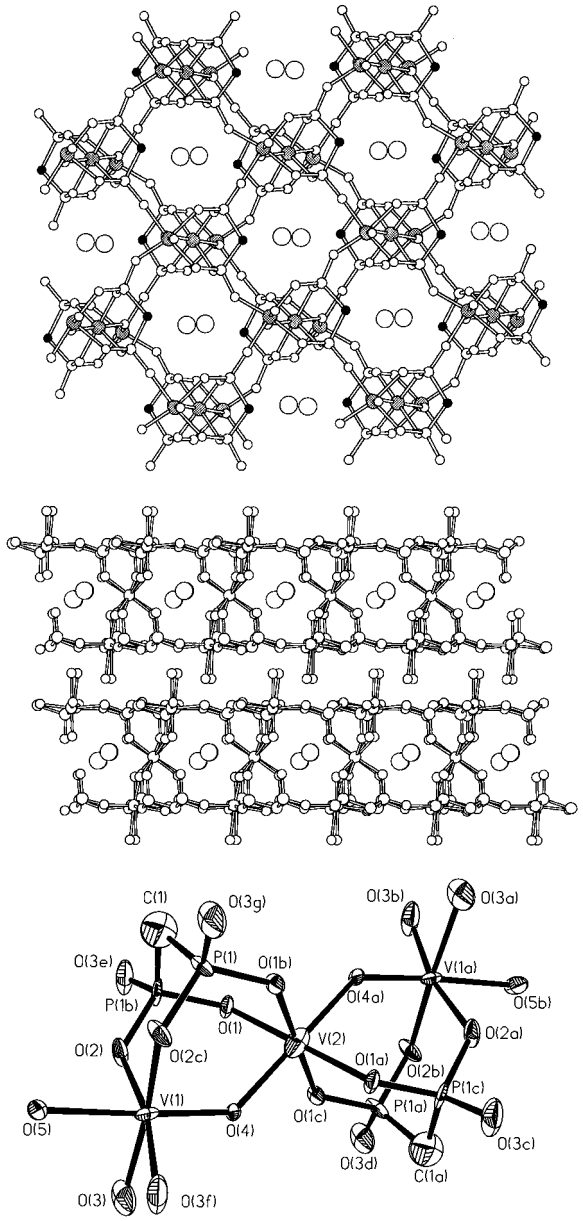

Figure 4. (a, top) View of the structure of $Cs[(VO)_2V(O_3PCH_2PO_3)_2(H_2O)_2]$ (**3**), along the *c* axis and normal to the layer plane, illustrating the *intralayer* cavities occupied by the Cs^+ cations. (b, middle) View of the structure of **3** parallel to the *a* axis and illustrating the occupancy of the interlamellar region by aquo-groups associated with the V(IV) sites of the trinuclear motifs which project into the space. (c, bottom) $\{V_3O_2(H_2O)_2(O_3PCH_2PO_3)_2\}$ unit which provides the fundamental structural motif in the design of the two-dimensional V—P—O framework of **3**.

V(III) center, the V—O bond lengths adopt a short−long−long−short pattern within each trinuclear unit: {V(IV)═O—V(III)—O═V(IV)}. Consequently, each V(IV) site projects an aquo group into the interlamellar region, resulting in layers three octahedra thick with top and bottom faces lined with aquo groups, producing a highly hydrophilic interlamellar region.

In a gross geometrical sense, the trinuclear core of **3** resembles a piece of the one-dimensional chain adopted by **2**. However, unlike the chain structures, where pendant {P═O} and/or {P—OH} units are observed, the {P—O} groups not involved in bonding within the trinuclear core of **3** are employed in bridging to adjacent trinuclear units. In this fashion, each trinuclear building block is linked to four adjacent trinuclear units in forming the two-dimensional network in a manner reminiscent of a Lego construction.

Table 10. Comparison of Structural Features of Vanadium−Organophosphate and Vanadium−Organodiphosphonate Phases

compound	structure type	vanadium motif	vanadium sites (oxidation state)	V=O_t[a,b]	V−$O_{phosphonate}$[c]	V−O_{other} (type)
$[H_2pip][VO(O_3PCH_2PO_3)]$	chain	isolated square pyramids	V1 (IV)	1.595(3)	1.980(2)(×4)	
$Cs[VO(HO_3PCH_2PO_3)]$	chain	corner-sharing octahedral chains	V1 (IV)	1.60(1)	2.00(1)(×4)	2.40(1) (bridging oxo)
$[VO(O_3PPh)(H_2O)]$	layer	corner-sharing octahedral chains	V1 (IV)	1.610(9)	1.96(1)(×3)	2.11(1) (aquo)
						2.14(1)(V···O=V)
$[(VO)_2(O_3PCH_2PO_3)_2(H_2O)_4]$	layer	isolated octahedra	V1 (IV)	1.606(3)	1.993(3)(×2)	2.103(4), (aquo, ×3)
			V2 (IV)	1.619(2)	2.021(3)(×4)	2.215(2) (aquo)
$(H_2en)[VO(O_3PCH_2CH_2PO_3)]$	layer	isolated square pyramids	V1 (IV)	1.586(6)	1.977(7)(×4)	
$(H_3NEt)_2[(VO)_3(O_3PPh)_4]$	layer	trinuclear units of corner-sharing octahedra	V1 (IV)	1.62(1)	1.981(8)(×4)	2.276(7) (V···O=V)
			V2 (IV)	1.638(9)	2.006(8)(×4)	2.162(9) (V···O=V)
$(H_2NEt_2)(H_2NMe_2)[(VO)_4(OH)_2(O_3PPh)_4]$	layer	binuclear units of corner-sharing pyramids	V1 (IV)	1.53(1)	1.958(9)(×3)	1.96(1) (hydroxy bridge)
$(Et_4N)[(VO)_3(OH)(H_2O)(O_3PC_2H_5)_3]\cdot H_2O$	layer	binuclear units of corner-sharing pyramids	V1 (IV)	1.54(1)	1.98(1)(×3)	1.96(1) (hydroxy bridge)
		isolated square pyramids	V3 (IV)	1.53(1)	1.97(1)(×3)	2.01(1) (aquo)
$Cs[(VO)_2V(O_3PCH_2PO_3)_2(H_2O)_2]$	layer	trinuclear unit of corner-sharing	V1, V2 (IV)		1.97(1)(×4)	1.783(9) (bridging oxo)
						2.14(1) (aquo)
		octahedra	V3 (III)	1.99(1)(×6)		
$(H_2pip)[(VO)_2(O_3PCH_2CH_2CH_2PO_3H)_2]$	stair-stepped	isolated square pyramids	V1 (IV)	1.585(6)	1.964(7)(×4)	
$[(VO)\{O_3PCH_2NH(C_2H_4)_2NHCH_2PO_3\}(H_2O)]$	"pillared" layers	isolated square pyramids	V1 (IV)	1.578(4)	2.008(3)(×4)	
$[H_2en][(VO)_4(OH)_2(H_2O)_2(O_3PCH_2CH_2CH_2PO_3)_2]\cdot 4H_2O$	"pillared" layers	binuclear units of corner-sharing octahedron and square pyramids	V1 (IV)	1.583(7)	1.971(8)(×3)	1.930(7) (bridging hydroxy)
			V2 (IV)	1.615(8)	1.993(8)(×3)	1.9995(7) (bridging hydroxy)
						2.388(9) (aquo)
$(H_3O)_2[(VO)V_2(OH)_2(O_3PCH_2CH_2PO_3)_2]\cdot H_2O$	"pillared" layers	chains of corner-sharing octahedra	V1, V2 (III)		1.981(7)(×4)	1.924(9) (hydroxy bridge ×2)
		isolated square pyramids	V3 (IV)		1.53(2)	1.95(1)(×4)
$(H_3O)[V_3(O_3PCH_2CH_2PO_3)(HO_3PCH_2CH_2PO_3H)_3]$	3-D	isolated octahedra	V1 (III)		2.00(1)(×6)	
$[V(HO_3PCH_2PO_3)(H_2O)]$	3-D	isolated octahedra	V1 (III)		1.982(6)(×4)	2.056(6) (aquo ×2)
			V2 (III)		2.015(6)(×6)	

[a] Esd's in parentheses; distances in angstroms. [b] Abbreviations: O_t, terminal oxo-group. [c] (×*n*), *n* refers to the number of ligands of a given type coordinated to the vanadium center.

The channels occupied by the Cs^+ cations result from rings formed by four adjacent trinuclear units of the two-dimensional networks. It is noteworthy that for layered vanadium−organophosphonate and vanadium−organodiphosphonate phases containing organoammonium cations, the cations invariably occupy interlamellar positions with respect to the V−P−O inorganic layers. The location of the Cs^+ cations in **3** was thus unexpected. However, the dimensions of the intralayer channels and the environment provided the Cs^+ cations in **3** are similar to those observed for the Cs^+ sites in the three-dimensional phases $CsVO(PO_4)$[39] and $Cs[V_2(PO_4)(HPO_4)_2(H_2O)_2]$.[40] In fact, the tightly packed layers of **3** render the interlamellar region inaccessible to cations of the dimensions of Cs^+. One consequence of the unique intralayer occupancy of the cations is this close approach of the layers, such that the aquo groups projecting from the surfaces of the slabs interleave in the interlamellar region.

While low-dimensional materials are common for metal−organophosphonate systems, three-dimensional phases are relatively rare, particularly for the organodiphosphonates which tend to partition into inorganic and organic domains. The structure of $[V(HO_3PCH_2PO_3)(H_2O)]$ (**4**) represents an unusual example of three-dimensional phase and an unique example of such a material with a neutral framework.

The framework of **4** is constructed from isolated $\{VO_6\}$ octahedra linked through methylenediphosphonate groups. As illustrated in Figure 5, there are two distinct V(III) coordination sites. The $\{VO_6\}$ octahedron of V(1) is defined by a pair of *trans* aquo ligands and four oxygen donors from each of four methylenediphosphonate groups. The octahedron about V(2) consists of oxygens from two methylenediphosphonate groups in the bidentate coordination mode and two adopting the monodentate type. Consequently, each methylenediphosphonate group bonds to two V(1) and two V(2) sites, through a total of five oxygen donors. The sixth oxygen is pendant and protonated, as confirmed by the P−O distance of 1.584(6) Å and consistent with charge requirements.

The connectivity pattern adopted by the V(III) octahedra and the $(HO_3PCH_2PO_3)^{3-}$ corner-sharing bitetrahedra results in a complex three-dimensional structure. A slice through the structure, shown in Figure 5, illustrates the unusual seven polyhedra rings, consisting of three $\{VO_6\}$ octahedra and four $\{O_3PC\}$ tetrahedra, which are formed. The pendant hydroxyl groups of the methylenediphosphonates and the aquo ligands are directed into these cavities.

Magnetic Properties. The magnetic susceptibility data for the compounds $Cs[VO(HO_3PCH_2PO_3)]$ (**2**) and $Cs[(VO)_2V(O_5PCH_2PO_3)_2(H_2O)_2]$ (**3**) exhibited Curie−Weiss behavior, and the magnetic data over the 1.7−300 K temperature range were analyzed according to eq 1.

$$\chi = C/(T - \Theta) = Ng^2\mu_B{}^2S(S+1)/[3k(T-\Theta)] \qquad (1)$$

The electron structure of the one-dimensional material $Cs[VO(HO_3PCH_2PO_3)]$ (**2**) corresponds to vanadium(IV) in the $3d^1$ electronic configuration. As shown in Figure 6, if the magnetic susceptibility data are corrected for the presence of a temperature independent paramagnetism (TIP), then the data may be fit to the Curie−Weiss law over the entire temperature range. The presence of the TIP term results in a slight curvature of the expected linear Curie−Weiss plot. The Curie−Weiss parameters are $C = 0.740$ (emu K)/mol, $\Theta = 1.9$ K, and TIP $= 0.0012$ emu/mol. The positive Θ corresponds to a weak ferromagnetic coupling between the vanadyl centers. Since the

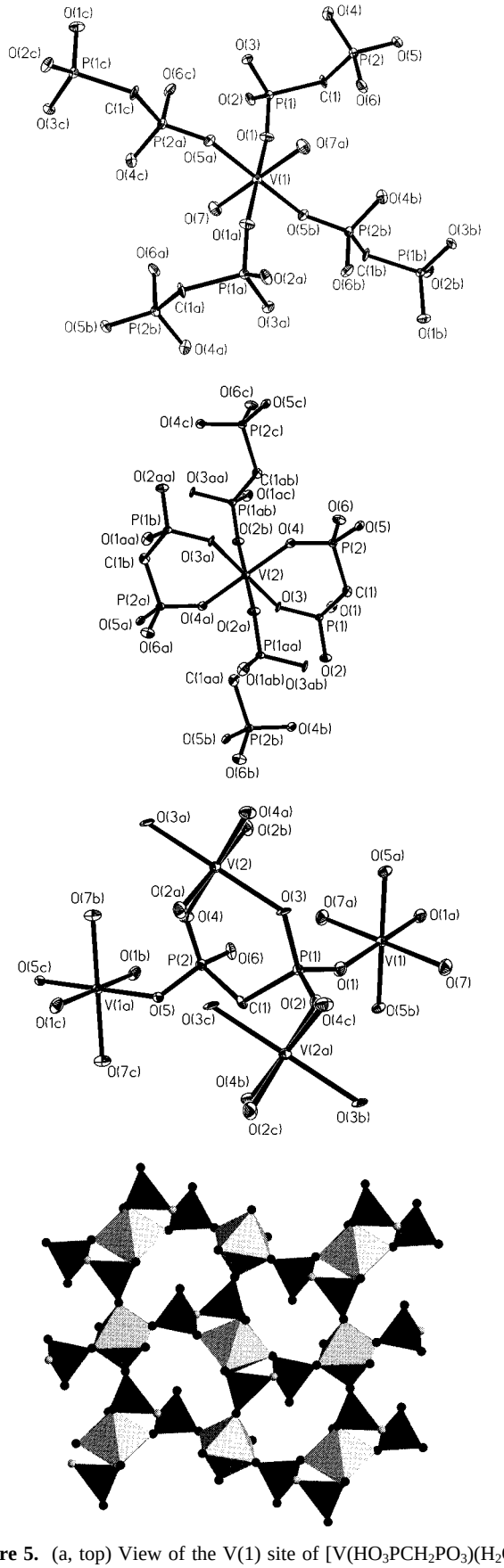

Figure 5. (a, top) View of the V(1) site of $[V(HO_3PCH_2PO_3)(H_2O)]$ (**4**). (b, second from the top) View of the V(2) site of **4**. (c, third from the top) View of the linking of V(1) and V(2) octahedra by the $\{HO_3PCH_2PO_3\}^{3-}$ group of **4**. (d, bottom) Polyhedral representation of the structure of **4**.

(39) Lii, K.-H.; Liu, W. C. *J. Solid State Chem.* **1993**, *103*, 38.
(40) Haushalter, H. C.; Wang, Z.; Thompson, M. E.; Zubieta, J. *Inorg. Chem.* **1993**, *32*, 3700.

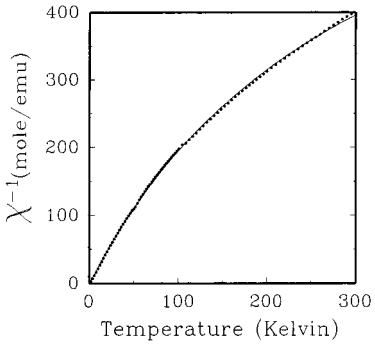

Figure 6. Inverse magnetic susceptibility of $Cs[VO(HO_3PCH_2PO_3)]$ (**2**), plotted as a function of temperature over the 1.7−300 K temperature region. The line drawn through the data is the fit to the Curie−Weiss model as described in the text.

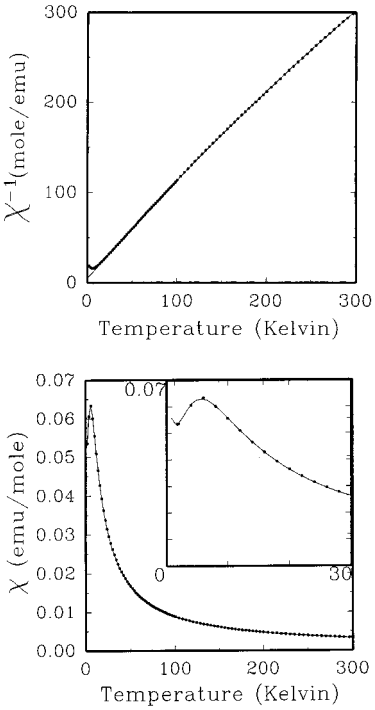

Figure 7. (a, top) Inverse magnetic susceptibility $[V(O_3PCH_2PO_3H)(H_2O)]$ (**4**), plotted as a function of temperature over the 1.7−300 K temperature region. The line drawn through the data is the fit to the Curie−Weiss model as described in the text. (b, bottom) Magnetic susceptibility of $[V(O_3PCH_2PO_3H)(H_2O)]$ (**4**), plotted as a function of temperature over the 1.7−300 K temperature region. The inset of the figure shows an expansion of the temperature region in the vicinity of the maximum. The curve drawn through the data is the fit to the binuclear model as described in the text.

structure of **2** consists of linear chains, this is a likely source for the coupling; however, the interaction is too weak to permit a thorough magnetic modeling of the linear chain behavior. For the $3d^1$ electronic structure of **2**, a *g*-value of 1.986 is obtained.

The magnetic behavior of **3** is likewise unexceptional, with least squares fitted parameters to eq 1 of $C = 2.305$ (emu K)/mol, $\Theta = 0.746$ K, and TIP = 0.000 373 emu/mol. The trinuclear units observed in the layer structure of **3** exhibit an electron structure corresponding to two vanadium(IV), $3d^1$, sites and a single vanadium(III), $3d^2$. The average *g*-value for this system is $g = 2.29$.

As shown in Figure 7, the temperature dependent susceptibility of $[V(HO_3PCH_2PO_3)(H_2O)]$ (**4**) exhibits a maximum consistent with short-range antiferromagnetic coupling. The magnetic susceptibility data for **4** were fit to eq 1 at higher temperatures ($T > 100$ K) with the fitted parameters $C = 0.912$ (emu K)/mol, $\Theta = -6.794$ K, and TIP = 0.000 323 emu/mol. Since the electron structure of **4** consists of V(III) ions with a $3d^2$, $S = 1$ electronic structure, the electrons may couple through a binuclear mechanism to give the characteristic maximum that is observed in the temperature dependent magnetic susceptibility. The magnetic exchange expected from V(III) ions is the isotropic Heisenberg−Dirac−Van Vleck Hamiltonian model, as shown in eq 2.

$$H = -2JS_1S_2 \tag{2}$$

Spin $S = 1$ systems have a very complicated solution to this problem that has been previously solved by Ginsberg and coworkers.[41] The resulting equation is quite lengthy and will be represented here as $\chi(g,J,D,zJ')$, where *D* is the zero field splitting that may occur in $S = 1$ systems, and zJ' is the molecular exchange field approximation for secondary magnetic interactions. Figure 7 shows the magnetic susceptibility data plotted as a function of temperature over the entire temperature range. The curve through the data represents the best least squares fit of the data to the $S = 1$ Heisenberg binuclear model with the following parameters: $g = 1.876$, $J/k = -2.48$ K, $D/k = -10.9$ K, $zJ'/k = 0.133$ K, and TIP = 0.000 43 emu/mol.

Observation and Conclusions

The structural versatility of the vanadium−organophosphonate system is rather remarkable, as illustrated by the entries in Table 10. Not only are one-, two-, and three-dimensional phases accessible, but the vanadium building blocks utilized in the construction of the solid span a compositional range from isolated polyhedra, to small oligomeric V−O−V bridged units, to infinite chains. This rich structural chemistry also reflects the occurrence of different vanadium coordination geometries and the accessibility of the V(IV) and V(III) oxidation states. Under the reducing conditions of the hydrothermal syntheses, the V(III) state is readily formed and contributes an octahedral building block which, in contrast to the V(IV) octahedra or square pyramids, contains no terminal {V═O} units and hence achieves six point connectivity within the V−P−O framework.

Further structural diversity is introduced upon condensation of the vanadium polyhedra with the organophosphonate or organodiphosphonate units. The phosphonate units may not only exhibit variable protonation patterns, such as RPO_3^{2-}, RPO_3H^-, $(O_3PR'PO_3)^{4-}$, $(HO_3PR'PO_3)^{3-}$, and $(HO_3PR'PO_3H)^{2-}$, giving rise to pendant {P−OH} groups, but also exhibit variable coordination modes to provide pendant {P═O} groups. In this fashion, a diphosphonate group may coordinate through as few as two oxygen donors or as many as six oxygen donors in the construction of the V−P−O connectivity pattern. A wide range of V−O−P bond angles can also be accommodated, allowing the linked polyhedra to form a variety of structural motifs.

The predominance of two-dimensional phases reflects the tendency of the structures to partition into inorganic and organic domains. This observation is illustrated by the structure of the prototype material $[VO(O_3PPh)(H_2O)]$ which may be described in terms of inorganic V−P−O layers alternating with organic $-C_6H_5$ double layers. The introduction of organodiphosphonate groups would be anticipated to provide similar structure types, i.e., −V−P−O layers pillared by the organic backbone of the diphosphonate linker. Consequently, the interlayer spacing should be amenable to variation by rational choice of tether substituents and tether lengths in the diphosphonate group. While this expectation has been realized in a number of instances listed

(41) Ginsberg, A. P.; Martin, R. L.; Brooks, R. W.; Sherwood, R. C. *Inorg. Chem.* **1972**, *12*, 2884.

in Table 10, it is also apparent that the element of rational design is elusive, as a variety of one-dimensional and three-dimensional materials may also be prepared, as well as 2-dimensional phases with unexpected network connectivities.

While the preparation of one-, two- and three-dimensional materials in the series $[H_2pip][VO(O_3PCH_2PO_3)]$, $[H_2en][VO(O_3PCH_2CH_2PO_3)]$, and $[H_2en][(VO)_4(OH)_2(H_2O)_2\ (O_3PCH_2CH_2CH_2PO_3)_2]\cdot 4H_2O$ suggested that phase dimensionality was subject to a measure of control through tether length manipulation, the structures of the materials of this study reveal that other factors, including cation identity and reaction conditions, are also determinants of product structure and composition.

While the templating role of the cation appears established in the preparation of these materials, the mechanism remains ambiguous, as one template can lead to different structures. Crystal-packing and charge-compensating effects are major determinants of cation incorporation into the solid lattice. Consequently, simple inorganic cations, such as Cs^+ and H_3O^+, may function as structure organizing constituents, as well as organoammonium cations. In certain instances, the V—P—O framework is neutral and cations are excluded altogether.

The preparations of the materials in Table 10 illustrate the power of hydrothermal synthesis in the preparation of materials by self-assembly from molecular precursors. Since these materials are metastable species, "designed" synthesis in the sense of predictability of product identity has not been achieved. On the other hand, by combining hydrothermal methods, suitable templates for framework organization, variations in reaction conditions (such as pH, fill volume, stoichiometries, temperature, etc.), and appropriate adjustments of organic spacers, functional groups, or steric requirements in the ligand component, it is possible to realize significant modifications of framework dimensionality, V—P—O layer separations, and compositional ranges of the product materials.

Acknowledgment. The work at Syracuse University was supported by NSF Grant CHE 9318824.

Supporting Information Available: Tables of structure determination details, atomic positional parameters, bond lengths, bond angles, anisotropic temperature factors, and calculated hydrogen atom positions for **1**−**4** (23 pages). Ordering information is given on any current masthead page.

IC960224B